THE JOURNAL OF PHYSICAL CHEMISTRY C

Article

pubs.acs.org/JPCC

Structural and Ionic Conduction Analyses of the $Na_2(Zr_{1-x}Al_x)O_{3-x/2}$ Solid Solution, During the CO_2 Chemisorption Process

Brenda Alcántar-Vázquez,[†,‡] J. Francisco Gómez-García,[§] Gustavo Tavizon,[§] Ilich A. Ibarra,[†] Cesar Diaz,[‡] Enrique Lima,[†] and Heriberto Pfeiffer*[,†]

[†]Instituto de Investigaciones en Materiales and [§]Facultad de Química, Universidad Nacional Autónoma de México, Del. Coyoacán, México DF, CP 04510, Mexico

[‡]Facultad de Ciencias Químicas e Ingeniería, Universidad Autónoma de Baja California, Tijuana, Baja California, CP 22390, Mexico

ABSTRACT: To determine the influence of the aluminum content in the sodium zirconate during the CO_2 chemisorption process, specific compositions in the $Na_2(Zr_{1-x}Al_x)O_{3-x/2}$ solid solution were produced. The synthesis was performed in order to restrict the aluminum crystalline sites to tetrahedral positions, substituting zirconium atoms. Samples were characterized using X-ray diffraction, N_2 adsorption−desorption and ^{27}Al solid-state nuclear magnetic resonance. Then, samples were tested as CO_2 captors using dynamic and isothermal analyses. Additionally, ionic conduction experiments were performed in different sodium containing phases to determine the effect of these phases in the CO_2 chemisorption process. Results showed that there are several factors that determine the CO_2 chemisorption in the pristine Na_2ZrO_3 and compounds of the $Na_2(Zr_{1-x}Al_x)O_{3-x/2}$ solid solution. Some of these factors are the presence or absence of different structural vacancies, as well as the presence of different phases in the carbonated external shell.

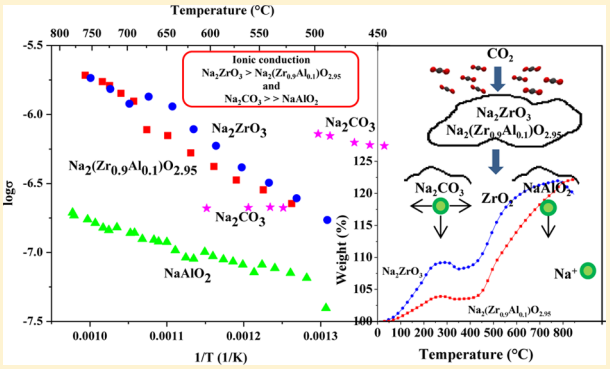

INTRODUCTION

Different alkaline ceramics show excellent CO_2 capture properties.[1−12] Some of these ceramics are lithium silicates (Li_8SiO_6, Li_4SiO_4, and Li_2SiO_3),[3,4,6,11,13−28] lithium aluminate (Li_5AlO_4),[2,29] lithium zirconate (Li_2ZrO_3),[5,30−44] sodium silicate (Na_2SiO_3),[45] and sodium zirconate (Na_2ZrO_3).[30,46−52] The CO_2 chemisorption mechanism on these ceramics has already been proposed. Initially, CO_2 chemisorption is produced over the ceramic surface, which implies that an external shell is formed. The external shell is composed of the corresponding alkaline carbonate (lithium or sodium carbonate), as well as alkaline secondary phases and/or metal oxides. Once the superficial CO_2 chemisorption is completed, the CO_2 chemisorption can be reactivated if the temperature is increased to promote different diffusion processes throughout the bulk of the material.[13,14,30−32,46−50,53]

Among all the lithium and sodium ceramics proposed as possible CO_2 captors, sodium zirconate (Na_2ZrO_3) seems to possess very good CO_2 capture properties, such as a wide temperature range of CO_2 chemisorption, good cyclability, and good kinetic properties, among others.[5,30,32,46−49,51,52] Na_2ZrO_3 has a monoclinic crystalline structure with lamellar building blocks, where sodium atoms are located among the $(ZrO_3)^{2-}$ layers, which favors sodium diffusion processes.[47] It has been proven that during the CO_2 capture on sodium or lithium ceramics, different diffusion processes are the limiting step of the whole reaction.[29,33,47,48,50,54] Thus, once the CO_2 chemisorption reaction covers the ceramic surface, an external shell is formed as it was previously mentioned. In the Na_2ZrO_3 case, the Na_2CO_3−ZrO_2 external shell possesses very interesting textural properties. The Na_2CO_3−ZrO_2 composite is mesoporous, when the reaction is produced at $T \leq 550$ °C. Consequently, the CO_2 chemisorption is not stopped, as CO_2 molecules can diffuse through these pores to reach the Na_2ZrO_3 fresh surface, continuing the CO_2 chemisorption process. Now, if the CO_2 chemisorption process is produced at temperatures higher than 550 °C, the Na_2CO_3−ZrO_2 external shell sinters, and the mesoporosity is no longer present. Thus, at $T > 550$ °C the CO_2 chemisorption is controlled by intercrystalline diffusion processes.[48]

In order to enhance the CO_2 chemisorption on these ceramics, different structural and/or chemical modifications have been carried out. For example, different solid solutions such as $Li_{2-x}Na_xZrO_3$, $Li_{3.7}Al_{0.1}SiO_4$, $Li_{3.7}Fe_{0.1}SiO_4$, and $Li_{4-x}Na_xSiO_4$[3,6,30,55] have been evaluated as possible CO_2 captors. In general, all these solid solutions have shown an improvement on different properties of the CO_2 chemisorption, for instance, efficiency and kinetic properties, in comparison to their respective pure alkaline ceramics. The improvements observed on the different solid solutions have been attributed to the point defect formation into the lattice or to the

Received: September 1, 2014
Revised: October 20, 2014
Published: October 21, 2014

secondary phase formation, and these improve diffusion processes, which are the limiting steps of the CO_2 capture.

In this respect, some thermodynamic considerations have been proposed. Thangadurai and Weppner[56] proposed the synthesis of the Li_4SiO_4 solid solution with different metal oxides having more negative Gibbs formation free energy (ΔG_f) than SiO_2. The metals reported were M = B, Al, Ga, and Cr. In all the cases, when the M−O bond attraction was increased, the Li−O interaction decreased, and consequently the lithium ion conductivity was improved. Later, Ortiz-Landeros et al.[12] used the same considerations to produce the $Li_{4+x}Si_{1-x}Al_xO_4$ solid solution. The solid solution compounds showed better CO_2 chemisorptions than pure Li_4SiO_4. Specifically, this solid solution importantly improved the CO_2 capture temperature range and efficiency. Therefore, if the same thermodynamic considerations are used for the Na_2ZrO_3, then the addition of aluminum must decrease the Na−O interaction, and consequently the CO_2 capture can be enhanced as the ΔG_f of Al_2O_3 (−1582.3 kJ/mol) is more negative than that of ZrO_2 (−1042.8 kJ/mol). Thus, the aim of the present work was to determine different diffusion processes on the $Na_2(Zr-Al)O_3$ system using structural, microstructural, and ionic conductivity techniques. The aluminum structural positions were evaluated, since it can be located at octahedral (sodium positions) or tetrahedral (zirconium positions) crystalline sites.

EXPERIMENTAL SECTION

Na_2ZrO_3 and nominal $Na_2(Zr_{0.9}Al_{0.1})O_{2.95}$ solid solution were synthesized via a solid-state reaction. Samples were obtained by mixing mechanically the stoichiometric amounts of zirconium oxide (ZrO_2, 98.0% Spectrum), sodium carbonate (Na_2CO_3, MCB lab), and aluminum nitrate ($Al(NO_3)_3$ $9H_2O$, 98.0% Aldrich), adding 10 wt % excess of sodium carbonate in all the cases to compensate for the sublimation effect.[50] Reagent mixtures were calcined at 900 °C for 6 h. It is worth mentioning that other compounds of the $Na_{2+x}(Zr_{1-x}Al_x)O_3$ solid solution ($Na_{2.1}(Zr_{0.9}Al_{0.1})O_3$ and $Na_{2.3}(Zr_{0.7}Al_{0.3})O_3$) were prepared and analyzed for comparison purposes, following the same synthesis procedure and the corresponding stoichiometric amounts.

The crystalline structure of the samples was determined by powder X-ray diffraction (XRD). Furthermore, ^{27}Al solid-state NMR experiments were evaluated to determine the aluminum distribution in all compositions of the solid solution. Solid-state NMR spectra were acquired on a Bruker Avance II spectrometer with a magnetic field strength of 7.05 T, corresponding to a ^{27}Al Larmor frequency of 78.3 MHz. Short single pulses ($\pi/12$) with a recycle time of 0.5 s were used. Samples were packed into zirconia rotors of 4 mm o.d. The ^{27}Al chemical shift was expressed as ppm from an aqueous solution of $Al(NO_3)_3$ as an external standard.

Microstructural properties of the materials were analyzed by N_2 adsorption−desorption, using a Minisorp II equipment from BEL Japan. N_2 adsorption−desorption isotherms were measured at 77 K, and before these experiments, samples were outgassed at room temperature for 24 h, under vacuum. The surface areas were calculated with the BET model. Then, different thermogravimetric CO_2 chemisorption experiments were performed using a thermobalance Q500HR, from TA Instruments. Initially, samples were dynamically heated from room temperature to 850 °C at 5 °C/min, using a CO_2 gas flow of 60 mL/min (Praxair, grade 3.0). Subsequently, a consecutive isothermal analysis was performed on the samples. Samples were heated to 200 °C and then this temperature was kept for 1 h. After that, the temperature was increased by 50 °C and isothermically treated for another hour. This procedure was continued up to 850 °C. It must be mentioned that all the samples were previously activated at 850 °C for 1 h in a N_2 (Praxair, 4.8 grade) flow before the CO_2 capture experiments were carried out.

In addition, ionic conductivity (σ) measurements were performed for different sodium phases involved in this chemisorption system (Na_2ZrO_3, $Na_2(Zr_{0.9}Al_{0.1})O_{2.95}$, Na_2CO_3, and $NaAlO_2$). For these experiments, fine grain powders of Na_2ZrO_3, $Na_2(Zr_{0.9}Al_{0.1})O_{2.95}$, Na_2CO_3, and $NaAlO_2$ were pressed in the form of pellets of about 1 cm in diameter and 0.1 cm in thickness. Then, each pellet was heated at the sintering temperature of each compound, and the top and bottom pellet surfaces were coated with gold (as oxygen-ion blocking electrode), using a sputtering technique. The pellets were separated in two sets according to their resistance: set number one for the high-resistance samples (Na_2ZrO_3 and $Na_2(Zr_{0.9}Al_{0.1})O_{2.95}$), and set number two for the higher-resistance samples ($NaAlO_2$ and Na_2CO_3). Measurements were performed in a quartz cell coupled to a vacuum system (800−700 mTorr) and heated between 400 and 800 °C. Both sample sets were analyzed using the two-point DC technique, with platinum wires as electrodes. In set number one a LakeShore 120 current source was used, with and an Agilent 34401A multimeter to measure the voltage drop, while in set number two a Keithley 6514 electrometer was employed.

RESULTS

Na_2ZrO_3 and $Na_2(Zr_{0.9}Al_{0.1})O_{2.95}$ solid solution were characterized by XRD (data not shown), and as it could be expected, both diffraction patterns matched with the 35−0770 JCPDS diffraction file, which corresponds to the monoclinic Na_2ZrO_3 crystalline phase. The presence of any other phase was not observed in those diffractograms and there were not significant differences between them.[50] After the crystalline verification of both samples, some microstructural properties were determined by N_2 adsorption−desorption (Figure 1). Both samples showed N_2 adsorption−desorption type II isotherms, with a very narrow H3-type hysteresis loop, according to the IUPAC classification.[57,58] This behavior corresponds to nonporous

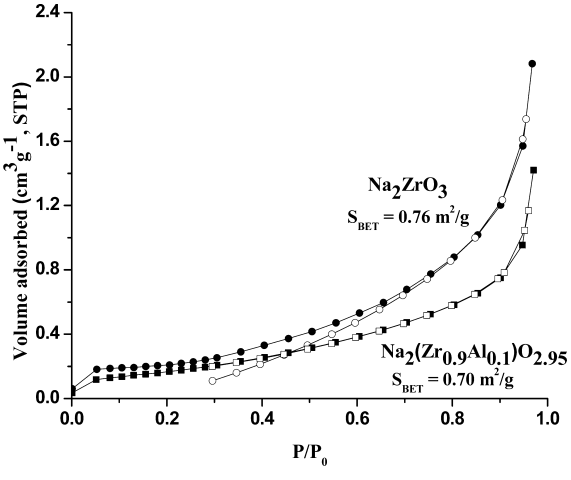

Figure 1. N_2 adsorption−desorption isotherms of the Na_2ZrO_3 and $Na_2(Zr_{0.9}Al_{0.1})O_{2.95}$ solid solution samples.

dx.doi.org/10.1021/jp508842e | J. Phys. Chem. C 2014, 118, 26212−26218

materials frequently obtained by solid state synthesis. Then, the surface areas were measured using the BET method, obtaining very similar values, ~0.7 m^2/g, in both cases.

After the characterization, dynamic thermogravimetric experiments were performed on Na_2ZrO_3 and $Na_2(Zr_{0.9}Al_{0.1})O_{2.95}$, using a CO_2 atmosphere. Initially, both samples depicted the typical CO_2 chemisorption behavior observed for Na_2ZrO_3,[30,47−50] with some important semiquantitative differences among them (Figure 2). At low temperatures (30−275 °C), samples presented an initial CO_2 chemisorption, which has been associated with a superficial process.[4,47−50] In fact, the initial chemisorption produces an external shell composed of Na_2CO_3 and ZrO_2. In addition, $NaAlO_2$ must be produced in the $Na_2(Zr_{0.9}Al_{0.1})O_{2.95}$ case. Between 275 and 400 °C there is a small desorption process (associated with the weight loss) followed of a lag period of time. These changes correspond to a dynamic superficial CO_2 chemisorption−desorption equilibrium. Finally, at T > 400 °C different diffusion processes are activated and the CO_2 chemisorption can continue through the particle bulk.[30,48,50]

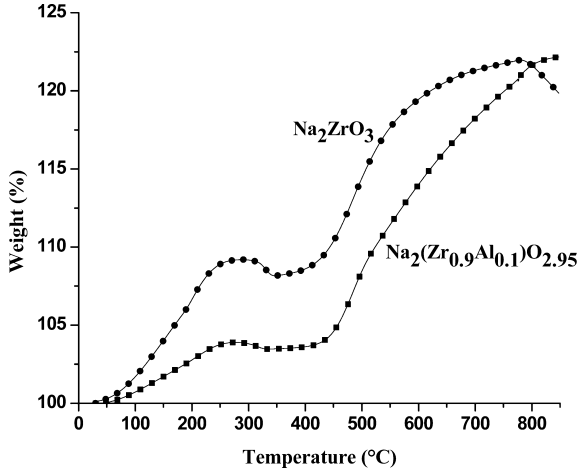

Figure 2. Dynamic thermogravimetric analysis of the Na_2ZrO_3 and $Na_2(Zr_{0.9}Al_{0.1})O_{2.95}$ solid solution samples in a CO_2 flow.

Although both samples presented the same general behavior, there were some important differences among them. At low temperatures, $T \leq 275$ °C, the CO_2 weight increment observed in the samples varied considerably. While Na_2ZrO_3 increased its weight in 9.2%, the $Na_2(Zr_{0.9}Al_{0.1})O_{2.95}$ sample captured only 3.8 wt % of CO_2. Additionally, the weight increment slopes of both curves were significantly different, in the same temperature range: 0.05 and 0.02 wt %/°C for Na_2ZrO_3 and $Na_2(Zr_{0.9}Al_{0.1})O_{2.95}$, respectively. This important difference cannot be explained in terms of the microstructural characteristics, as both samples presented very similar surface areas (0.7 m^2/g). Additionally, it has been reported that aluminum addition into the Na_2ZrO_3 structure increases the CO_2 capture at low temperatures,[50] which seemed to be a contradictory result. In this previous report,[50] the samples were structurally different to those presented herein, as the aluminum atoms were randomly located in sodium (octahedral coordination) and zirconium (tetrahedral coordination) crystalline positions producing different Na_2ZrO_3 structural defects, which are represented according to the following Kröger−Vink notation:

$$Na_2ZrO_3 \xrightarrow{(x/2)Al_2O_3} (Na_{2-3x}Al_x)ZrO_3 \rightarrow Na_{Na} + Al^{\cdot\cdot}_{Na} + 2V'_{Na} + Zr_{Zr} + O_o \quad (1)$$

$$Na_2ZrO_3 \xrightarrow{(x/2)Al_2O_3} Na_2(Zr_{1-x}Al_x)O_{3-x/2} \rightarrow Na_{Na} + Zr_{Zr} + Al'_{Zr} + 1/2V^{\cdot\cdot}_O + O_O \quad (2)$$

However, in the present Al-containing Na_2ZrO_3 solid-solution ($Na_2(Zr_{0.9}Al_{0.1})O_{2.95}$) the ^{27}Al solid-state NMR results showed a different structural organization. Figure 3 shows that $Na_2(Zr_{0.9}Al_{0.1})O_{2.95}$ only presents one NMR peak located at around 68 ppm, which corresponds to the tetrahedral coordination.[59] In other words, aluminum atoms are only located at the zirconium crystalline positions.

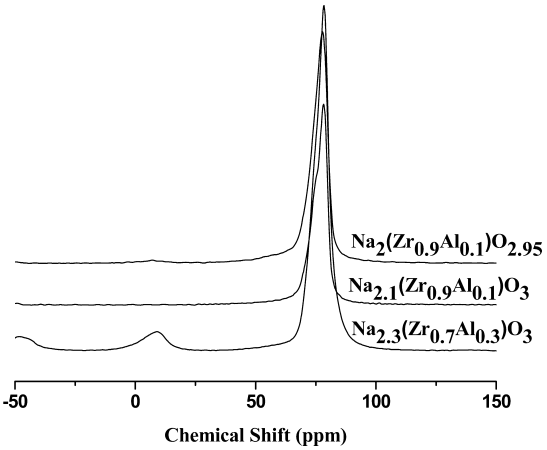

Figure 3. ^{27}Al solid state NMR spectra of the $Na_2(Zr_{0.9}Al_{0.1})O_{2.95}$ $Na_{2.1}(Zr_{0.9}Al_{0.1})O_3$ and $Na_{2.3}(Zr_{0.7}Al_{0.3})O_3$ solid solutions.

Therefore, only the second Kröger−Vink reaction must apply in the present sample. This structural variation may have induced the CO_2 capture decrement observed at low temperatures on the $Na_2(Zr_{0.9}Al_{0.1})O_{2.95}$ sample, in comparison to the previously reported samples. It seems that sodium vacancies play an important role in the CO_2 chemisorption at low temperatures.

To corroborate this hypothesis, other two samples were prepared: $Na_{2.1}(Zr_{0.9}Al_{0.1})O_3$ and $Na_{2.3}(Zr_{0.7}Al_{0.3})O_3$. These solid solution compounds were synthesized seeking to reduce the presence of sodium vacancies, but at the same time increasing the aluminum substitution at the zirconium crystalline positions. Figure 3 shows the ^{27}Al solid-state RMN spectra of these samples. It is clearly evident that $Na_2(Zr_{0.9}Al_{0.1})O_{2.95}$ (the initial compound) and $Na_{2.1}(Zr_{0.9}Al_{0.1})O_3$ only present an ^{27}Al NMR peak at around 68 ppm, which corresponds to the tetrahedral coordination. Thus, the aluminum atoms are located at zirconium crystalline positions. However, in the $Na_{2.3}(Zr_{0.7}Al_{0.3})O_3$ case, a second ^{27}Al NMR weak peak appeared at 5 ppm, which indicates that a few aluminum atoms are located at the sodium crystalline positions (octahedral coordination[59]). In these cases the first Kröger−Vink reaction may be the most appropriate. Nevertheless, another possibility is shown by the following Kröger−Vink equation, in which there is not any kind of vacancy, but interstitial sodium atoms are produced:

dx.doi.org/10.1021/jp508842e | J. Phys. Chem. C 2014, 118, 26212−26218

$$Na_2ZrO_3 \xrightarrow{(x/2)(Al_2O_3+Na_2O)} Na_{2+x}(Zr_{1-x}Al_x)O_3 \rightarrow Na_{Na} + Na_i + Zr_{Zr} + Al'_{Zr} + O_O \quad (3)$$

Figure 4 shows the CO_2 capture thermograms of these four samples between 30 and 275 °C. As it could be expected, the

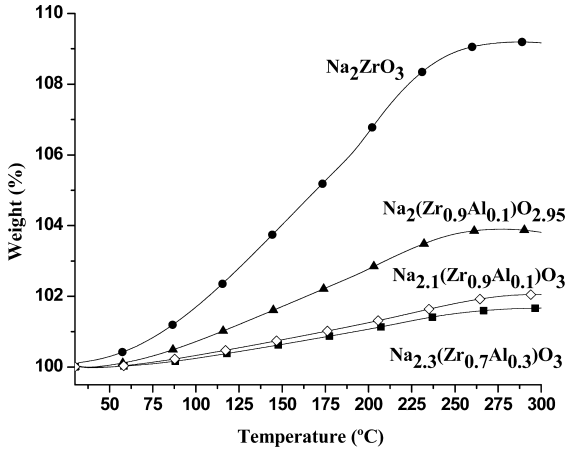

Figure 4. Dynamic thermogravimetric analysis of the Na_2ZrO_3, $Na_2(Zr_{0.9}Al_{0.1})O_{2.95}$, $Na_{2.1}(Zr_{0.9}Al_{0.1})O_3$, and $Na_{2.3}(Zr_{0.7}Al_{0.3})O_3$ solid solutions in a CO_2 flow.

CO_2 chemisorption decreased at low temperatures, as follows: Na_2ZrO_3 > $Na_2(Zr_{0.9}Al_{0.1})O_{2.95}$ > $Na_{2.1}(Zr_{0.9}Al_{0.1})O_3$ > $Na_{2.3}(Zr_{0.7}Al_{0.3})O_3$. This can be explained in two ways. First, if the third Kröger–Vink reaction occurs, the absence of sodium vacancies reduces the CO_2 chemisorption, although the total sodium amount increased, as interstitial sodium atoms were produced. It must be pointed out that the corresponding solid solutions, previously reported,[50] with aluminum atoms at tetrahedral and octahedral positions, presented the highest CO_2 chemisorption at low temperatures, but in those cases the presence of octahedrally coordinated aluminum was importantly higher than in the present $Na_{2.3}(Zr_{0.7}Al_{0.3})O_3$ sample, confirming the relevance of the vacancies on the CO_2 chemisorption process in this temperature range. Conversely, if the aluminum atoms were located in tetrahedral positions, the oxygen vacancies might increase (reaction 2), as well as the mobility of sodium atoms, but the $NaAlO_2$ amounts would also increase in the external shell, limiting the CO_2 chemisorption.

Coming back to Figure 2, in the second temperature range (275–400 °C) there is a small CO_2 desorption process (associated with the weight loss). The weight loss corresponds to a thermal shift of the dynamic CO_2 chemisorption–desorption equilibrium. Before the desorption process, Na_2ZrO_3 had chemisorbed more CO_2 than $Na_2(Zr_{0.9}Al_{0.1})O_{2.95}$, and consequently it desorbed more CO_2 as well. In this case, the desorption process does not depend on the original Na_2ZrO_3 structure or defects, as it is produced from the new external shell composed of ZrO_2, Na_2CO_3, and $NaAlO_2$ in the $Na_2(Zr_{0.9}Al_{0.1})O_{2.95}$ case.

Finally, it has been reported that at T > 400 °C different diffusion processes are activated and the CO_2 chemisorption can continue through the Na_2CO_3–ZrO_2 external shell and the Na_2ZrO_3.[33,47,48,50] However, in the $Na_2(Zr_{0.9}Al_{0.1})O_{2.95}$ sample, the external shell contains $NaAlO_2$ in addition to ZrO_2 and Na_2CO_3 (see reactions 4 and 5), which modifies the diffusion processes.

$$Na_2ZrO_3 + CO_2 \rightarrow Na_2CO_3 + ZrO_2 \quad (4)$$

$$Na_2(Zr_{0.9}Al_{0.1})O_{2.95} + 0.95CO_2 \rightarrow 0.95Na_2CO_3 + 0.9ZrO_2 + 0.1NaAlO_2 \quad (5)$$

Therefore, in order to corroborate the CO_2 chemisorption behavior, Na_2ZrO_3 and $Na_2(Zr_{0.9}Al_{0.1})O_{2.95}$ samples were isothermically analyzed consecutively between 200 and 850 °C as a function of time (Figure 5). As it could be expected, the

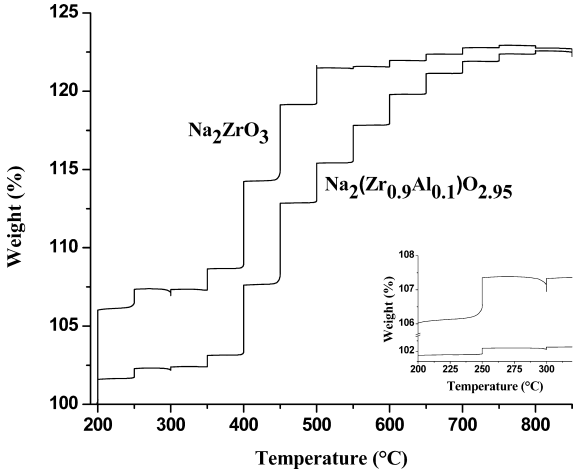

Figure 5. Consecutive isothermal analyses of the Na_2ZrO_3 and $Na_2(Zr_{0.9}Al_{0.1})O_{2.95}$ solid solution samples in a CO_2 flow.

CO_2 chemisorbed in Na_2ZrO_3 was always higher than that in $Na_2(Zr_{0.9}Al_{0.1})O_{2.95}$. Between 200 and 450 °C the CO_2 capture behavior was very similar to those observed in the dynamic TG experiments (Figure 2), where the CO_2 chemisorption–desorption equilibrium was detected even at 300 °C (see inset in Figure 5). Nevertheless, the Na_2ZrO_3 consecutive and isothermal experiments presented an evident discontinuity between 550 and 600 °C, associated with a very slight weight loss, although its corresponding dynamic thermogram presented a smooth exponential weight increment in the same temperature range. This effect can be associated with microstructural changes produced in the Na_2CO_3–ZrO_2 external shell during CO_2 chemisorption of Na_2ZrO_3. It has been reported that the Na_2CO_3–ZrO_2 external shell contains mesoporous, when it is produced at T < 500 °C. However, if the CO_2 chemisorption process is produced at $T \geq$ 550 °C, the Na_2CO_3–ZrO_2 external shell sinters, and the mesoporosity disappears.[48] Therefore, in the present case, as the consecutive and isothermal experiment allows to certain CO_2 chemisorption equilibrium degree, when the Na_2CO_3–ZrO_2 external shell sinters a partial CO_2 desorption must be produced. Something else must be pointed out: this effect was not observed on the $Na_2(Zr_{0.9}Al_{0.1})O_{2.95}$ sample because the presence of $NaAlO_2$ in the external shell is considered to change the microstructural thermal evolution. Thus, $NaAlO_2$ may inhibit the mesoporosity formation.

To confirm that $NaAlO_2$ modifies the carbonated external shell, the $Na_2(Zr_{0.9}Al_{0.1})O_{2.95}$ sample, treated isothermally at 500 °C in a CO_2 flow, was analyzed by N_2 adsorption to determine the surface area, as the Na_2ZrO_3 material presents one of the highest mesoporosities at this temperature.[48] However, for $Na_2(Zr_{0.9}Al_{0.1})O_{2.95}$, the BET surface area was equal to 0.4 m^2/g. Therefore, the surface area decreased from

dx.doi.org/10.1021/jp508842e | J. Phys. Chem. C 2014, 118, 26212–26218

0.7 to 0.4 m^2/g, instead of increasing.[48] Because the solid solution particles are considered nonporous, the BET area corresponds selectively to the external shell and these results confirm that $NaAlO_2$ modifies the microstructure evolution of the external shell.

In the results presented here, it has been shown that structural (vacancies and atomic crystalline arranges) and microstructural effects are very important factors in CO_2 chemisorption. However, there are several papers related to alkaline ceramics showing that the CO_2 chemisorption can be modified by diffusive processes, where the presence of different lithium secondary phases can increase or decrease the bulk reactivity.[1,12,32,34] In the lithium ceramic cases, the external shell is composed of Li_2CO_3 and different lithium secondary phases, where the presence of each lithium secondary phase can enhance or decrease the CO_2 chemisorption, depending on their lithium diffusion coefficients.[1] Based on this statement, the ionic conductivity of the following sodium phases was analyzed: Na_2ZrO_3, $Na_2(Zr_{0.9}Al_{0.1})O_{2.95}$, Na_2CO_3, and $NaAlO_2$. If the electronic contribution to conductivity is neglected, and the blocking electrode is taken into account, ionic conductivity will be proportional to the sodium diffusion in compounds.

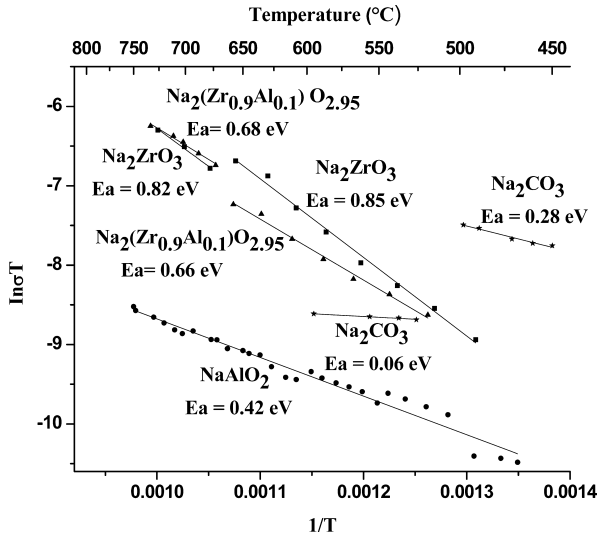

Figure 6. Arrhenius plots of the ionic conductivity for the Na_2ZrO_3, $Na_2(Zr_{0.9}Al_{0.1})O_{2.95}$, $NaAlO_2$, and Na_2CO_3 samples.

Figure 6 shows the Arrhenius plot ($\ln \sigma T$ v $1/T$, eq 6), where the activation energy of the ionic conduction process can be determined.

$$\ln \sigma T = -\left(\frac{E_a}{K_B}\right)\left(\frac{1}{T}\right) + \ln A \qquad (6)$$

where σ is the ionic conductivity (S cm^{-1}), T is the temperature (K), E_a is the activation energy (eV), K_B is the Boltzmann constant (8.617×10^{-5} eV/K) and A is the pre-exponential constant.

Figure 6 shows the temperature dependence of the ionic conductivity for the Na_2ZrO_3, $Na_2(Zr_{0.9}Al_{0.1})O_{2.95}$, $NaAlO_2$, and Na_2CO_3 samples. As it could be expected, all the phases presented a higher ionic conduction as a function of temperature, except for the Na_2CO_3, in which the ionic conductivity decreases between 520 and 595 °C. This is associated with a Na_2CO_3 crystalline phase transition, from monoclinic (at low temperature) to hexagonal (at high temperature).[60] From this figure, it can be seen that the ionic conductivity decreases as follows in the sodium zirconate and aluminate phases: $Na_2ZrO_3 > Na_2(Zr_{0.9}Al_{0.1})O_{2.95} \gg NaAlO_2$. Therefore, the sodium ionic conduction must be favored in the pristine zirconate phase without aluminum. Additionally, the carbonate external shell is composed of $NaAlO_2$ and Na_2CO_3. In this case, if the sodium ionic conduction in the $NaAlO_2$ phase is compared with that of the Na_2CO_3 phase, it is clearly evident that sodium ionic conduction is considerably lower in the $NaAlO_2$ phase.

Na_2ZrO_3, $Na_2(Zr_{0.9}Al_{0.1})O_{2.95}$, and Na_2CO_3 phases presented two well-defined slopes as a function of temperature, while $NaAlO_2$ only presents one slope in the whole temperature range. Na_2ZrO_3 and $Na_2(Zr_{0.9}Al_{0.1})O_{2.95}$ presented activation energy changes at around 660 °C. This ionic conduction change is in good agreement with different studies, which have shown that at similar temperatures the CO_2 capture process in Na_2ZrO_3 becomes mainly controlled by intercrystalline diffusion processes.[48] Additionally, the activation energies calculated for these ceramics, in the whole temperature range, decrease as follows: $Na_2ZrO_3 > Na_2(Zr_{0.9}Al_{0.1})O_{2.95} > NaAlO_2 > Na_2CO_3$. In other words, it seems that sodium diffusion is more easily activated in $Na_2(Zr_{0.9}Al_{0.1})O_{2.95}$ than in Na_2ZrO_3. This is also in good agreement with the initial ΔG_f thermodynamic theory,[56] which establishes that the Na−O bond is weaker in the aluminum containing solid solutions. However, the activation energy of $NaAlO_2$ is higher than that of Na_2CO_3. So, as soon as the external shell is produced, sodium diffusion must be limited by the $NaAlO_2$ phase.

Thermogravimetric CO_2 chemisorption results showed that it decreases with the aluminum addition in Na_2ZrO_3, when the Al atoms are located only at tetrahedral positions, although the activation energy of $Na_2(Zr_{0.9}Al_{0.1})O_{2.95}$ is smaller than that of Na_2ZrO_3. Therefore, the vacancy deficiency and $NaAlO_2$ formation must be mainly responsible for the observed drop in CO_2 chemisorption, as the CO_2 chemisorption process is controlled by diffusion processes, and this is usually the limiting step of the whole reaction process. To summarize, kinetic diffusion produced in the carbonate external shell controls the whole CO_2 chemisorption process.

CONCLUSIONS

Na_2ZrO_3 and $Na_2(Zr_{1-x}Al_x)O_{3-x/2}$ solid solution were prepared by solid state reaction. The analysis performed by ^{27}Al NMR confirmed that aluminum atoms are totally incorporated in tetrahedral crystalline positions, occupying zirconium positions. Na_2ZrO_3 and $Na_2(Zr_{1-x}Al_x)O_{3-x/2}$ samples were able to chemisorb CO_2 in a wide temperature range, but Na_2ZrO_3 presented higher CO_2 chemisorption than the solid solution compounds. The differences observed produced by the absence of cationic vacancies, as the aluminum atoms are only at zirconium positions. In these cases, the CO_2 capture decreased as a function of the aluminum content as follows: $Na_2ZrO_3 > Na_2(Zr_{0.9}Al_{0.1})O_{2.95} > Na_{2.1}(Zr_{0.9}Al_{0.1})O_3 > Na_{2.3}(Zr_{0.7}Al_{0.3})O_3$. Therefore, the reduction of sodium vacancies must decrease the CO_2 chemisorption, although the total sodium amount increased, as interstitial sodium atoms.

Additionally, sodium ionic conductivity of different phases was analyzed to complement the CO_2 chemisorption mechanism in Na_2ZrO_3 and $Na_2(Zr_{1-x}Al_x)O_{3-x/2}$. The analyzed

dx.doi.org/10.1021/jp508842e | J. Phys. Chem. C 2014, 118, 26212−26218

phases were as follows: Na_2ZrO_3 and $Na_2(Zr_{0.9}Al_{0.1})O_{2.95}$ as initial chemisorbents, as well as Na_2CO_3 and $NaAlO_2$ as the different sodium phases produced in the external shell. The ionic conductivity and activation energy of the $Na_2(Zr_{0.9}Al_{0.1})O_{2.95}$ are smaller than those in Na_2ZrO_3. This result was is in good agreement with the initial ΔG_f thermodynamic theory, establishing that the Na−O bond must become weaker in the aluminum containing compounds. However, if the ionic conductivity activation energy of $NaAlO_2$ and Na_2CO_3 (sodium phases present at the external shell) are compared, the activation energy in the $NaAlO_2$ case is higher than that in Na_2CO_3. Thus, the ionic conductivity processes in the external shell are limited by the $NaAlO_2$ presence.

AUTHOR INFORMATION

Corresponding Author

*Phone: +52 (55) 5622 4627, Fax: +52 (55) 56161371, E-mail: pfeiffer@iim.unam.mx.

Notes

The authors declare no competing financial interest.

ACKNOWLEDGMENTS

This work was financially supported by the projects PAPIIT-UNAM (IN-102313). Authors thank to A. Tejeda and G. Zedillo for technical help.

REFERENCES

(1) Ortiz-Landeros, J.; Ávalos-Rendón, T.; Gómez-Yáñez, C.; Pfeiffer, H. Analysis and Perspectives Concerning CO_2 Chemisorption on Lithium Ceramics Using Thermal Analysis. *J. Therm. Anal. Calorim.* **2012**, *108*, 647−655.

(2) Ávalos-Rendón, T.; Casa-Madrid, J.; Pfeiffer, H. Thermochemical Capture of Carbon Dioxide on Lithium Aluminates ($LiAlO_2$ and Li_5AlO_4): A New Option for the CO_2 Absorption. *J. Phys. Chem. A* **2009**, *113*, 6919−6923.

(3) Mejia-Trejo, V.; Fregoso-Israel, E.; Pfeiffer, H. Textural, Structural, and CO_2 Chemisorption Effects Produced on the Lithium Orthosilicate by its Doping with Sodium ($Li_{4-x}Na_xSiO_4$). *Chem. Mater.* **2008**, *20*, 7171−7176.

(4) Mosqueda, H.; Vazquez, C.; Bosch, P.; Pfeiffer, H. Chemical Sorption of Carbon Dioxide (CO_2) on Lithium Oxide (Li_2O). *Chem. Mater.* **2006**, *18*, 2307−2310.

(5) Nair, B.; Burwood, R.; Goh, V.; Nakagawa, K.; Yamaguchi, T. Lithium Based Ceramics Materials and Membranes for High Temperature CO_2 Separation. *Prog. Mater. Sci.* **2009**, *54*, 511−541.

(6) Gauer, C.; Heschel, W. Doped Lithium Orthosilicate for Absorption of Carbon Dioxide. *J. Mater. Sci.* **2006**, *41*, 2405−2409.

(7) Olivares-Marín, M.; Castro-Díaz, M.; Drage, T.; Maroto-Valer, M. Use of Small Amplitude Oscillatory Shear Rheometry to Study the Flow Properties of Pure and Potassium-Doped Li_2ZrO_3 Sorbents during the Sorption of CO_2 at High Temperatures. *Sep. Purif. Technol.* **2010**, *73*, 415−420.

(8) Pacciani, R.; Torres, J.; Solsona, P.; Coe, C.; Quinn, R.; Hufton, J.; Golden, T.; Vega, L. F. Influence of the Concentration of CO_2 and SO_2 on the Absorption of CO_2 by a Lithium Orthosilicate-Based Absorbent. *Environ. Sci. Technol.* **2011**, *45*, 7083−7088.

(9) Xiao, Q.; Tang, X.; Liu, Y.; Zhong, Y.; Zhu, W. Citrate Route to Prepare K-Doped Li_2ZrO_3 Sorbents with Excellent CO_2 Capture Properties. *Chem. Eng. J.* **2011**, *174*, 231−235.

(10) Xiao, Q.; Liu, Y.; Zhong, Y.; Zhu, W. A Citrate Sol-Gel Method to Synthesize Li_2ZrO_3 Nanocrystals with Improved CO_2 Capture Properties. *J. Mater. Chem.* **2011**, *21*, 3838−3842.

(11) Rodríguez-Mosqueda, R.; Pfeiffer, H. Thermokinetic Analysis of the CO_2 Chemisorption on Li_4SiO_4 by Using Different Gas Flow Rates and Particle Sizes. *J. Phys. Chem. A* **2010**, *114*, 4535−4541.

(12) Ortiz-Landeros, J.; Gomez-Yañez, C.; Palacios-Romero, L.; Lima, E.; Pfeiffer, H. Structural and Thermochemical Chemisorption of CO_2 on $Li_{4+x}(Si_{1-x}Al_x)O_4$ and $Li_{4-x}(Si_{1-x}V_x)O_4$ Solid Solutions. *J. Phys. Chem. A* **2012**, *116*, 3163−3171.

(13) Kato, M.; Nakagawa, K.; Essaki, K.; Maezawa, Y.; Takeda, S.; Kogo, R.; Hagiwara, Y. Novel CO_2 Absorbents Using Lithium-Containing Oxide. *Int. J. Appl. Ceram. Technol.* **2005**, *2*, 467−475.

(14) Nakagawa, K.; Ohashi, T. A Novel Method of CO_2 Capture from High Temperature Gases. *J. Electrochem. Soc.* **1998**, *145*, 1344−1346.

(15) Kato, M.; Yoshikawa, S.; Nakagawa, K. Carbon Dioxide Absorption by Lithium Orthosilicate in a Wide Range of Temperature and Carbon Dioxide Concentrations. *J. Mater. Sci. Lett.* **2002**, *21*, 485−487.

(16) Venegas, M. J.; Fregoso-Israel, E.; Pfeiffer, H. Kinetic and Reaction Mechanism of CO_2 Sorption on Li_4SiO_4: Study of the Particle Size Effect. *Ind. Eng. Chem. Res.* **2007**, *46*, 2407−2412.

(17) Okumura, T.; Enomoto, K.; Togashi, N.; Oh-Ishi, K. CO_2 Absorption Reaction of Li_4SiO_4 Studied by the Rate Theory Using Thermogravimetry. *J. Ceram. Soc. Jpn.* **2007**, *115*, 491−497.

(18) Escobedo-Bretado, M.; Guzmán-Velderrain, V.; Lardizabal-Gutierrez, D. A New Synthesis Route to Li_4SiO_4 as CO_2 Catalytic/Sorbent. *Catal. Today* **2005**, *107−108*, 863−867.

(19) Essaki, K.; Nakagawa, K.; Kato, M.; Uemoto, H. CO_2 Absorption by Lithium Silicate at Room Temperature. *J. Chem. Eng. Jpn.* **2004**, *37*, 772−777.

(20) Essaki, K.; Kato, M.; Uemoto, H. Influence of Temperature and CO_2 Concentration on the CO_2 Absorption Properties of Lithium Silicate Pellets. *J. Mater. Sci.* **2005**, *18*, 5017−5019.

(21) Khomane, R. B.; Sharma, B.; Saha, S.; Kulkarni, B. D. Reverse Microemulsion Mediated Sol−Gel Synthesis of Lithium Silicate Nanoparticles under Ambient Conditions: Scope for CO_2 Sequestration. *Chem. Eng. Sci.* **2006**, *61*, 3415−3418.

(22) Kato, M.; Nakagawa, K. New Series of Lithium Containing Complex Oxides, Lithium Silicates, for Application as a High Temperature CO_2 Absorbent. *J. Ceram. Soc. Jpn.* **2001**, *109*, 911−914.

(23) Yamaguchi, T.; Niitsuma, T.; Nair, B. N.; Nakagawa, K. Lithium Silicate Based Membranes for High Temperature CO_2 Separation. *J. Membr. Sci.* **2007**, *294*, 16−21.

(24) Kalinkin, A. M.; Kalinkina, E. V.; Zalkind, O. A.; Makarova, T. I. Mechanochemical Interaction of Alkali Metal Metasilicates with Carbon Dioxide: 1. Absorption of CO_2 and Phase Formation. *Colloid J.* **2008**, *70*, 33−41.

(25) Kalinkin, A. M.; Kalinkina, E. V.; Zalkind, O. A. Mechanochemical Interaction of Alkali Metal Metasilicates with Carbon Dioxide: 2. the Influence of Thermal Treatment on the Properties of Activated Samples. *Colloid J.* **2008**, *70*, 42−47.

(26) Shan, S. Y.; Jia, Q. M.; Jiang, L. H.; Li, Q. C.; Wang, Y. M.; Peng, J. H. Novel Li_4SiO_4-Based Sorbents from Diatomite for High Temperature CO_2 Capture. *Ceram. Int.* **2013**, *39*, 5437−5441.

(27) Qi, Z.; Daying, H.; Yang, L.; Qian, Y.; Zibin, Z. Analysis of CO_2 Sorption/Desorption Kinetic Behaviors and Reaction Mechanism on Li_4SiO_4. *AIChE J.* **2013**, *59*, 901−911.

(28) Durán-Muñoz, F.; Romero-Ibarra, I. C.; Pfeiffer, H. Analysis of the CO_2 Chemisorption Reaction Mechanism in Lithium Oxosilicate (Li_8SiO_6): A New Option for High-Temperature CO_2 Capture. *J. Mater. Chem. A* **2013**, *1*, 3919−3925.

(29) Ávalos-Rendon, T.; Lara, V. H.; Pfeiffer, H. CO_2 Chemisorption and Cyclability Analyses of Lithium Aluminate Polymorphs (α-and β-Li_5AlO_4). *Ind. Eng. Chem. Res.* **2012**, *51*, 2622−2630.

(30) Pfeiffer, H.; Vazquez, C.; Lara, V.; Bosch, P. Thermal Behavior and CO_2 Absorption of $Li_{2-x}Na_xZrO_3$ Solid Solutions. *Chem. Mater.* **2007**, *19*, 922−926.

(31) Ida, J.; Xiong, R.; Lin, J. Y. S. Synthesis and CO_2 Sorption Properties of Pure and Modified Lithium Zirconate. *Sep. Purif. Technol.* **2004**, *36*, 41−51.

(32) Ida, J.; Lin, J. Y. S. Mechanism of High-Temperature CO_2 Sorption on Lithium Zirconate. *Environ. Sci. Technol.* **2003**, *37*, 1999−2004.

(33) Martínez-dlCruz, L.; Pfeiffer, H. Effect of Oxygen Addition on the Thermokinetic Properties of CO_2 Chemisorption on Li_2ZrO_3. *Ind. Eng. Chem. Res.* **2010**, *49*, 9038−9042.
(34) Pfeiffer, H.; Bosch, P. Thermal Stability and High-Temperature Carbon Dioxide Sorption on Hexa-Lithium Zirconate ($Li_6Zr_2O_7$). *Chem. Mater.* **2005**, *17*, 1704−1710.
(35) Xiong, R.; Ida, J.; Lin, Y. Kinetics of Carbon Dioxide Sorption on Potassium-Doped Lithium Zirconate. *Chem. Eng. Sci.* **2003**, *58*, 4377−4385.
(36) Nakagawa, K.; Ohashi, T. A Reversible Change between Lithium Zirconate and Zirconia in Molten Carbonate. *J. Electrochem. Soc.* **1999**, *67*, 618−621.
(37) Hwang, K. S.; Lee, Y. H.; Hwangbo, S. Preparation of Lithium Zirconate Nanopowder Prepared by Electrostatic Spraying for CO_2 Sorbent. *Mater. Sci. Polym.* **2007**, *25*, 969−975.
(38) Nair, B.; Yamaguchi, T.; Kawamura, H.; Nakao, S.; Nakagawa, K. Processing of Lithium Zirconate for Applications in Carbon Dioxide Separation: Structure and Properties of the Powders. *J. Am. Ceram. Soc.* **2004**, *87*, 68−74.
(39) Yi, K.; Eriksen, D. Low Temperature Liquid State Synthesis of Lithium Zirconate and its Characteristics as a CO_2 Sorbent. *Sep. Sci. Technol.* **2006**, *41*, 283−296.
(40) Ochoa-Fernández, E.; Rusten, H. K.; Jakobsen, H. A.; Rønning, M.; Holmen, A.; Chen, D. Sorption Enhanced Steam Methane Reforming Using Li_2ZrO_3 as Sorbent: Sorption Kinetics and Reactor Simulation. *Catal. Today.* **2005**, *106*, 41−46.
(41) Ochoa-Fernández, E.; Rønning, M.; Grande, T.; Chen, D. Nanocrystalline Lithium Zirconate with Improved Kinetics for High Temperature CO_2 capture. *Chem. Mater.* **2006**, *18*, 1383−1385.
(42) Ochoa-Fernández, E.; Rønning, M.; Grande, T.; Chen, D. Synthesis and CO_2 Capture Properties of Nanocrystalline Lithium Zirconate. *Chem. Mater.* **2006**, *18*, 6037−6046.
(43) Ochoa-Fernández, E.; Rønning, M.; Yu, X.; Grande, T.; Chen, D. Compositional Effects of Nanocrystalline Lithium Zirconate on its CO_2 Capture Properties. *Ind. Eng. Chem. Res.* **2008**, *47*, 434−442.
(44) Iwana, A.; Stephensonb, H.; Ketchiec, W.; Lapkin, A. High Temperature Sequestration of CO_2 using Lithium Zirconates. *Chem. Eng. J.* **2009**, *146*, 249−258.
(45) Rodríguez-Mosqueda, R.; Pfeiffer, H. High CO_2 Capture in Sodium Metasilicate (Na_2SiO_3) at Low Temperatures (30−60 °C) Through the CO_2−H_2O Chemisorption Process. *J. Phys. Chem. C* **2013**, *117*, 13452−13461.
(46) López-Ortiz, A.; Perez-Rivera, N. G.; Reyes, A.; Lardizabal-Gutierrez, D. Novel Carbon Dioxide Solid Acceptors using Sodium Containing Oxides. *Sep. Sci. Technol.* **2004**, *39*, 3559−3572.
(47) Alcérreca-Corte, I.; Fregoso-Israel, E.; Pfeiffer, H. CO_2 Absorption on Na_2ZrO_3: A Kinetic Analysis of the Chemisorption and Diffusion Processes. *J. Phys. Chem. C* **2008**, *112*, 6520−6525.
(48) Martínez-dlCruz, L.; Pfeiffer, H. Microstructural Thermal Evolution of the Na_2CO_3 Phase Produced during a Na_2ZrO_3−CO_2 Chemisorption Process. *J. Phys. Chem. C* **2012**, *116*, 9675−9680.
(49) Santillan-Reyes, G. G.; Pfeiffer, H. Analysis of the CO_2 Capture in Sodium Zirconate (Na_2ZrO_3). Effect of the Water Vapor Addition. *Int. J. Greenhouse Gas Control* **2011**, *5*, 1624−1629.
(50) Alcántar-Vázquez, B.; Diaz, C.; Romero-Ibarra, I. C.; Lima, E.; Pfeiffer, H. Structural and CO_2 Chemisorption Analyses on $Na_2(Zr_{1-x}Al_x)O_3$ Solid Solutions. *J. Phys. Chem. C* **2013**, *117*, 16483−16491.
(51) Zhao, T.; Ochoa-Fernández, E.; Ronning, M.; Chen, D. Preparation and High- Temperature CO_2 Capture Properties of Nanocrystalline Na_2ZrO_3. *Chem. Mater.* **2007**, *19*, 3294−3301.
(52) Martínez-dlCruz, L.; Pfeiffer, H. Cyclic CO_2 Chemisorption−Desorption Behavior of Na_2ZrO_3: Structural, Microstructural and Kinetic Variations Produced as a Function of Temperature. *J. Solid State Chem.* **2013**, *204*, 298−304.
(53) *Advances in CO_2 Conversion and Utilization*; Yun-Hang, H., Ed.; ACS Symposium Series 1056; American Chemical Society: Washington, DC, 2010.
(54) Ortiz-Landeros, J.; Romero-Ibarra, I. C.; Gómez-Yañez, C.; Lima, E.; Pfeiffer, H. $Li_{4+x}(Si_{1-x}Al_x)O_4$ Solid Solution Mechanosynthesis and Kinetic Analysis of the CO_2 Chemisorption Process. *J. Phys. Chem. A* **2013**, *117*, 6303−6311.
(55) Pfeiffer, H.; Lima, E.; Bosch, P. Lithium-Sodium Metazirconate Solid Solutions, $Li_{2-x}Na_xZrO_3$ ($0 \leq X \leq 2$), a Hierarchical Architecture. *Chem. Mater.* **2006**, *18*, 2642.
(56) Thangadurai, V.; Weppner, W. Solid-State Lithium Ionic Conductors: Design Considerations by Thermodynamic Approach. *Ionics* **2002**, *8*, 281−292.
(57) Lowell, S.; Shields, J. E.; Thomas, M. A. *Characterization of Porous Solids and Powders: Surface Area, Pore Size and Density; Particle Technology Series*; Kluwer Academic Publishers: London, 2004.
(58) McCash, E. M. *Surface Chemistry*; Oxford University Press: Oxford, U.K., 2002.
(59) Bastow, T. J.; Hobday, M. E.; Smith, M. E.; Whitfield, H. J. Structural characterization of Na_2ZrO_3. *Solid State Nucl. Magn. Reson.* **1994**, *3*, 49−57.
(60) Swainsonf, I. P.; Dovet, M. T.; Harrisfill, M. J. Neutron powder diffraction study of the ferroelastic phase transition and lattice melting in sodium carbonate, Na_2CO_3. *J. Phys.: Condens. Matter* **1995**, *7*, 4395−4417.